Analytic approach to the optical response of one-dimensional photonic crystal slabs

Kazuki Koshino*
Frontier Research System, The Institute of Physical and Chemical Research (RIKEN), Hirosawa 2-1, Wako, Saitama 351-0198, Japan
(Received 29 May 2002; revised 2 December 2002; published 30 April 2003)

We investigate the optical response of one-dimensional photonic crystal slabs for an incident wave from free space. The Maxwell equation is solved in an analytic manner using the eigenmodes for the empty lattice case (without periodic gratings), and compact formulas for transmittivity of the incident wave and excitation efficiency of waveguide modes are obtained. These formal results are visualized at certain parameters. The effect of width in the wave vector of incident wave is also discussed.

DOI: 10.1103/PhysRevB.67.165213 PACS number(s): 42.70.Qs, 42.82.Et

I. INTRODUCTION

By comparison of Maxwell and Schrödinger equations, it is known that regions with large dielectric constant for electromagnetic wave correspond to regions with low potential for particles.[1] Thus, a plain slab of dielectric supports two kinds of eigenmodes; (i) waveguide modes, which are spatially bound in the normal direction to the slab (which we hereafter call the z direction) almost within the thickness of the slab, and (ii) radiation modes, which extend infinitely in the z direction. In the case of a plain slab structure, there is no coupling between waveguide modes and radiation modes, so the existence of waveguide modes does not affect the incident wave from the z direction.

Due to recent progress of fabricating nanostructures, we are able to prepare such artificial slabs whose dielectric constant is periodically modulated in one or two directions within the plane of the slab, which are called photonic crystal slabs (PCS).[2–6] In this system, contrary to a plain dielectric slab, the in-plane wave vector is not conserved, because infinitesimal translation symmetry in the in-plane directions is lost by the variance of the dielectric constant. Instead, the periodic modulation introduces the coupling between the modes satisfying the Bragg's condition. This mechanism enables the externally incident wave from the z direction to interact with those waveguide modes that are folded back into the light cone,[7] which brings unique optical features to the PCS's.

One of the typical consequences of the coupling to the waveguide modes is the appearance of sharp dips in the transmission spectrum of the incident wave from the z direction. This has been observed experimentally[8,9] and also has been reproduced by solving the Maxwell equation in a numerical manner.[9–11] By using such numerical methods, one can obtain numerical values of many quantities (transmissivity, spatial distribution of EM field, and so on) with high accuracy. However, the underlying physical mechanisms are buried in the huge processes in numerical calculations. It is impossible to see transparently the dependence of these physical quantities on the structural and dielectric parameters of the PCS, and, therefore, to give compact guidelines for designing the PCS's. Thus, analytic approaches are desired where physical quantities are given as functions of the parameters of the PCS.

A well-known approach to handling the waveguide modes analytically is the coupled-mode theories.[12–14] In these theories, the main concern is laid in the energy exchange among several waveguide modes, and the interaction between the waveguide mode and the radiation modes is not treated rigorously. Apparently, such theories are not suitable to discuss the optical response of PCS's to the EM wave incident from the z direction, because the incident wave belongs to the radiation modes. Recently, Ochiai *et al.* have treated the coupling ν between the waveguide and radiation modes by perturbation,[6] and derived nonphenomenological expressions for the energy and radiative width of the waveguide modes. However, as a result of perturbative treatment, the theory cannot describe the nonperturbative quantities in ν, such as the transmissivity of the incident wave and the amplitudes of the waveguide modes excited by the incident wave.

In this study, we discuss the optical response of PCS by showing the analytic solution of the Maxwell equation, which has a nonperturbative form in the coupling constant ν. In order to obtain the solution, we utilize the fact that the photonic modes in the PCS can be regarded as a typical example of a Fano-type problem, which is characterized by the linear coupling between discrete levels (the waveguide modes that are folded back into the light cone by periodic gratings) and continua (radiation modes), and employ an approximation by taking into account only those modes that are almost resonant to the incident wave. In particular, we demonstrate the solution in the simplest situation, where the frequency of the incident wave is low enough so that it is not diffracted into other radiation modes, and therefore only a single continuum of radiation modes should be taken into account. The solution clearly reveals the underlying mechanism for how the structural and dielectric parameters of the PCS are reflected in the optical response. We also show how the optical response of an ideal PCS is altered in realistic cases.

The composition of this paper is as follows: in Sec. II, the structure of the PCS considered in this study is described. In Sec. III, the Maxwell equation is solved for incidence of infinite plane wave. After decomposing the electric field by eigenmodes for the empty lattice case, the equation is treated as a Fano-type problem[15] with two discrete levels and a continuum, which allows analytic solution of the Maxwell equation. The formal results are visualized with numerical examples. In Sec. IV, we discuss the effect of finite width in the in-plane wave vector of incident wave, which is inevitable in

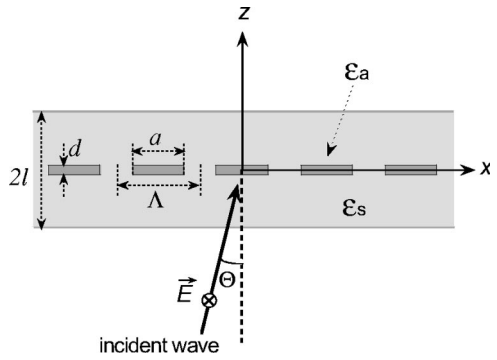

FIG. 1. Section of the system on the x-z plane. The system is uniform in the y direction (perpendicular to paper). The incident light has its wave vector $(P,0,Q)$ and is TE polarized.

real experimental situations. The results are summarized in Sec. V.

II. SYSTEM

The structure of the PCS that we discuss in this study is described in this section. The system is composed of a plain slab of transparent dielectric (dielectric constant: ϵ_s), incorporated with a one-dimensional array of stripes of different dielectric (dielectric constant: ϵ_a), as sketched in Fig. 1.

We decompose the dielectric function into two parts as $\epsilon(x,z)=\epsilon_1(z)+\epsilon_2(x,z)$. $\epsilon_1(z)$ is the dielectric function of the slab without periodicity in the x direction, which is given by

$$\epsilon_1(z)=\begin{cases}\epsilon_s+(\epsilon_a-\epsilon_s)a/\Lambda & (|z|<d/2)\\ \epsilon_s & (d/2<|z|<l)\\ 1 & (l<|z|),\end{cases} \tag{1}$$

where d and a are the thickness and width of the stripes, Λ is the periodicity of the arrays, and l is half of the thickness of the slab. On the other hand, $\epsilon_2(x,z)$ denotes periodic modulation of the dielectric function, which is given by

$$\epsilon_2(x,z)=\begin{cases}(\epsilon_a-\epsilon_s)[X(x)-a/\Lambda] & (|z|<d/2)\\ 0 & (d/2<|z|),\end{cases} \tag{2}$$

where $X(x)$ is a periodic function of x with period Λ, which is given, for $|x|<a/2$, by

$$X(x)=\begin{cases}1 & (|x|<a/2)\\ 0 & (a/2<|x|<\Lambda/2).\end{cases} \tag{3}$$

The reason for this particular decomposition is to let $\int_{-\Lambda/2}^{\Lambda/2}dx\,\epsilon_2(x,z)$ be zero for later convenience. For simplicity, we substitute the step function with width d at $z=0$ by a delta function $d\,\delta(z)$, and employ the following forms of $\epsilon_1(z)$ and $\epsilon_2(x,z)$;[16]

$$\epsilon_1(z)=\begin{cases}\epsilon_s+(\epsilon_a-\epsilon_s)(a/\Lambda)d\,\delta(z) & (|z|<l)\\ 1 & (l<|z|),\end{cases} \tag{4}$$

$$\epsilon_2(x,z)=(\epsilon_a-\epsilon_s)[X(x)-a/\Lambda]d\,\delta(z). \tag{5}$$

As for the incident electromagnetic wave, we consider a situation where the wave vector $(P,0,Q)$ of the incident wave lies on the x-z plane and there is no field variation in the y direction. P and Q are related to the wave number K and the incident angle Θ by $P=K\sin\Theta$ and $Q=K\cos\Theta$. In this case, the field is separated into TE and TM modes. We discuss the TE-polarized case in the following.

III. SOLUTION FOR INFINITE PLANE WAVE INCIDENCE

A. Eigenmode expansion

In this section, we solve the Maxwell equation with the dielectric function $\epsilon_1(x)+\epsilon_2(x,z)$, for incidence of TE-polarized infinite plane wave with wave vector $(P,0,Q)$. In TE-polarized cases, electromagnetic field is completely described by the y component of the electric field, which we denote by $E(x,z)$ in the following; x and z components of the magnetic field are given by $B_x=i(cK)^{-1}\partial_z E(x,z)$ and $B_z=-i(cK)^{-1}\partial_x E(x,z)$. The fundamental equation to solve is the Maxwell equation for $E(x,z)$:

$$[\partial_x^2+\partial_z^2+K^2\{\epsilon_1(z)+\epsilon_2(x,z)\}]E(x,z)=0. \tag{6}$$

In order to solve Eq. (6), we use the eigenmodes for the empty lattice case, i.e., $\epsilon_2(x,z)=0$, which are easily accessible due to one-dimensionality. The eigenmodes are divided as follows:

$$L^{-1/2}e^{ipx}f_{pq\sigma}(z), \tag{7}$$

where L is the quantization length, and a real function $f_{pq\sigma}(z)$ satisfies the following equation:

$$[\mathrm{d}_z^2+(p^2+q^2)\epsilon_1(z)-p^2]f_{pq\sigma}(z)=0, \tag{8}$$

and is normalized by

$$\int_{-L/2}^{L/2}\mathrm{d}z\,\epsilon_1(z)f_{pq\sigma}(z)f_{pq'\sigma'}(z)=\delta_{qq'}\delta_{\sigma\sigma'}. \tag{9}$$

As is well known, the eigenmodes for the empty lattice case are classified into radiation modes and waveguide modes. The radiation modes have three independent indices p (x component of the wave vector), q (z component of the wave vector, outside of the slab), and σ (parity for the z direction; $\sigma=\oplus$ or $\ominus$). Contrarily, as for the waveguide modes, q and σ are automatically determined as functions of p. We shall therefore omit the indices q and σ for the waveguide modes in the following.

We expand the electric field by the eigenmode functions as

$$E(x,z)=\sum_{p,q,\sigma}\tilde{b}_{pq\sigma}L^{-1/2}e^{ipx}f_{pq\sigma}(z), \tag{10}$$

which leads to the following equations among the coefficients:

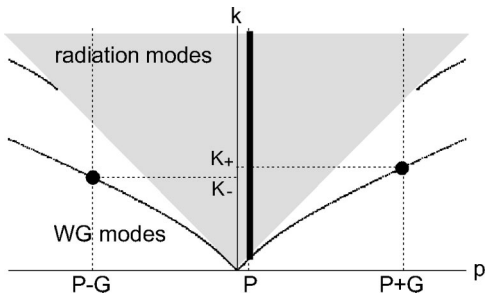

FIG. 2. Energy of eigenmodes for a plain slab, plotted against p (x component of the wave vector). Continuum of radiation modes (gray region) lie inside the light cone, while the branches of waveguide modes (curves) are outside of it. In this study, radiation modes with $p=P$ (thick line) and a pair of waveguide modes with $p=P\pm G$ (dots) are taken into account.

$$(K^2-p^2-q^2)\tilde{b}_{pq\sigma}+K^2 l\sum_{q',\sigma',j(\neq 0)}\nu_j f_{pq\sigma}(0)f_{(p+jG)q'\sigma'}(0)\times\tilde{b}_{(p+jG)q'\sigma'}=0, \tag{11}$$

where $G=2\pi/\Lambda$, j runs over nonzero integers, and ν_j is a dimensionless coupling constant defined by

$$\nu_j=(\epsilon_a-\epsilon_s)(d/l)\frac{\sin(j\pi a/\Lambda)}{j\pi}. \tag{12}$$

Because the incorporated materials are located at $z=0$, the interaction takes place only among the even parity modes ($\sigma=\oplus$), and those with odd parity remain eigenmodes even in existence of the periodic modulation $\epsilon_2(x,z)$.

B. Treatment as Fano problem

Now it is apparent from Eq. (11) that the incident wave ($p=P$) is coupled only to those modes with $P+jG$. It should be stressed here that the incident wave can interact with the waveguide modes through this mechanism, which results in distinct dips in the transmission spectrum. In this study, we restrict ourselves to the simplest case where the wave number of the incident wave is small and diffraction into other radiation modes ($p=P\pm G,P\pm 2G,\ldots$) does not occur. The condition is expressed by $(P-G)^2>P^2+Q^2$ or, in terms of K and Θ, $K/G<(1-\sin\Theta)/\cos^2\Theta$. In this low frequency region, the relevant modes are the continuum of radiation modes $\tilde{b}_{Pq\oplus}$ with $p=P$ (thick line in Fig. 2), and a pair of waveguide modes $\tilde{b}_{P\pm G}$ belonging to the lowest branch (two dots in Fig. 2). It should be remarked again that the waveguide modes have only one index p after fixing the branch. Thus, we treat this problem as a Fano-type one[15] with two discrete states and one continuum. The crucial interactions are (i) those between $\tilde{b}_{Pq\oplus}$ and $\tilde{b}_{P\pm G}$ (characterized by ν_1), which couple the incident wave to waveguide modes and also give radiative widths to the waveguide modes, and (ii) those between $\tilde{b}_{P+G}$ and $\tilde{b}_{P-G}$ (characterized by ν_2), which is important because these two waveguide modes are energetically degenerate for a normal incidence ($\Theta=0$). Taking into account these two kinds of interaction, and using the following abbreviated notations, $b_\pm=l^{1/2}\tilde{b}_{P\pm G}$, $b_q=(L/2\pi)^{1/2}\tilde{b}_{Pq\oplus}$, $f_\pm=l^{1/2}f_{P\pm G}(0)$, $f_q=(L/2\pi)^{1/2}f_{Pq\oplus}(0)$, and $K_\pm$ (the frequencies of waveguide modes $b_{P\pm G}$, see Fig. 2), we get the following homogeneous equations:

$$(Q^2-q^2)b_q+\nu_1 f_q K^2(f_+b_++f_-b_-)=0, \tag{13}$$

$$(K^2-K_+^2)b_++\nu_2 f_+f_-K^2b_-+\nu_1 f_+lK^2\int_0^\infty dq f_q b_q=0, \tag{14}$$

$$(K^2-K_-^2)b_-+\nu_2 f_+f_-K^2b_++\nu_1 f_-lK^2\int_0^\infty dq f_q b_q=0. \tag{15}$$

If one wants to extend the theory to larger wave number region, other modes should be taken into account additionally. For example, for $(1-\sin\Theta)/\cos^2\Theta<K/G<(1+\sin\Theta)/\cos^2\Theta$, the continuum of radiation modes with $p=P-G$ should also be considered.

C. Forms of $b_\pm$ and b_q

After the simplified treatment described in the previous subsection, the problem has been reduced to coupled linear equations (13), (14), and (15). From Eq. (13), we get

$$b_q=\nu_1K^2(f_+b_++f_-b_-)\frac{f_q}{q+Q}\left[\mathrm{P}\left(\frac{1}{q-Q}\right)+\eta\delta(q-Q)\right], \tag{16}$$

where P means taking the principal part on integration, and η is a dimensionless constant to be determined in the following. Substituting Eq. (16) into Eqs. (14) and (15), we get simultaneous equations for (b_+,b_-). From the condition that the equations have nonzero solutions for (b_+,b_-), we obtain

$$\int_0^\infty dq\frac{f_q^2}{q+Q}\left[\mathrm{P}\left(\frac{1}{q-Q}\right)+\eta\delta(q-Q)\right]=-\frac{(K^2-K_+^2)(K^2-K_-^2)-\nu_2^2f_+^2f_-^2K^4}{\nu_1^2lK^4[(f_+^2+f_-^2-2\nu_2f_+^2f_-^2)K^2-f_+^2K_-^2-f_-^2K_+^2]}, \tag{17}$$

and b_+/b_- is given by

$$\frac{b_+}{b_-}=\frac{f_+[(1-\nu_2f_-^2)K^2-K_-^2]}{f_-[(1-\nu_2f_+^2)K^2-K_+^2]}. \tag{18}$$

η is determined through Eq. (17). On evaluation of left-hand side of Eq. (17), we substitute f_q in the integrand by f_Q, neglecting its q dependence.[17] Then η is immediately given by

$$\eta=-\frac{2Q[(K^2-K_+^2)(K^2-K_-^2)-\nu_2^2f_+^2f_-^2K^4]}{\nu_1^2lK^4f_Q^2[(f_+^2+f_-^2-2\nu_2f_+^2f_-^2)K^2-f_+^2K_-^2-f_-^2K_+^2]}. \tag{19}$$

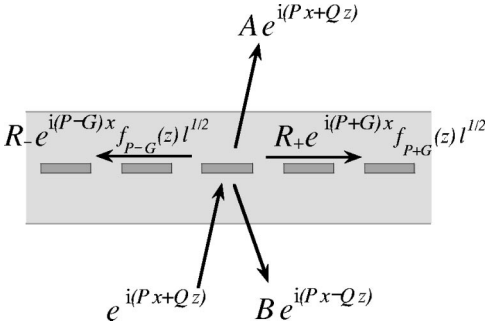

FIG. 3. Summary of the solution for incidence of infinite plane wave. The amplitudes A, B, and $R_\pm$ are given in Eqs. (23), (24), and (25). $f_{P\pm G}(z)$ is a function almost confined in the thickness of the slab.

It should be remarked that $f_\pm$, $K_\pm$, and f_Q are dependent upon P. Thus η and b_+/b_- are given as functions of the incident wave vector $(P,0,Q)$, or, equivalently, (K,Θ). If the incorporated material is dispersive, ν_j may also depend on K through the dielectric constant $\epsilon_a(K)$.

D. Amplitudes of the transmitted wave, reflected wave, and excited waveguide modes

Using Eqs. (10), (16), and (A1), the even-parity solution of Eq. (6) outside of the slab is given by

$$E_{PQ\oplus}(x,z)=\frac{\nu_1(f_+b_++f_-b_-)K^2}{(\pi L)^{1/2}}e^{iPx}\int_0^\infty dq\,\frac{f_q}{q+Q}\times\left[\mathrm{P}\left(\frac{1}{q-Q}\right)+\eta\delta(q-Q)\right]\cos(q|z|+\theta_{Pq\oplus}),\tag{20}$$

where $\theta_{Pq\oplus}$ is a phase shift associated with the eigenmodes for the empty lattice case (see Appendix A). Substituting f_q and $\theta_{Pq\oplus}$ in the integrand by f_Q and $\theta_{PQ\oplus}$, Eq. (20) leads at $|z|\to\infty$:

$$E_{PQ\oplus}(x,z)=\left(\frac{\eta^2+\pi^2}{\pi L}\right)^{1/2}\frac{\nu_1(f_+b_++f_-b_-)f_QK^2}{2Q}\times e^{iPx}\cos(Q|z|+\theta_{PQ\oplus}+\phi),\tag{21}$$

where ϕ $(0\leqslant\phi\leqslant\pi)$ is defined by

$$\phi=\cos^{-1}(\eta/\sqrt{\eta^2+\pi^2}).\tag{22}$$

Thus, an additional phase shift ϕ is introduced in the even-parity solution. In order to satisfy the boundary condition that there is no wave propagating in the $(P,0,-Q)$ direction in $l<z$, an odd-parity solution $E_{PQ\ominus}\propto L^{-1/2}e^{iPx}f_{PQ\ominus}(z)$ should be superposed on the even-parity solution $E_{PQ\oplus}$.

The result is summarized in Fig. 3. For incidence of infinite plane wave of $e^{i(Px+Qz)}$, the amplitudes (including phases) of the transmitted wave, reflected wave, and excited waveguide modes are given, respectively, by

$$A=\cos(\theta_{PQ\oplus}-\theta_{PQ\ominus}+\phi)e^{i(\theta_{PQ\oplus}+\theta_{PQ\ominus}+\phi)},\tag{23}$$

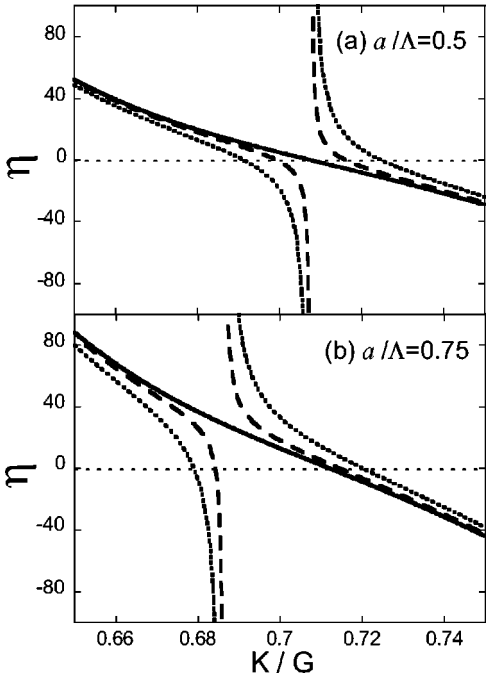

FIG. 4. Plot of $\eta(K)$ at incident angles $\Theta=0°$ (solid curve), $\Theta=1°$ (broken curve), and $\Theta=2°$ (dotted curve). The parameters are chosen as follows; $\epsilon_s=2$, $\epsilon_a=10$, $d/l=0.02$, $\Lambda/l=1$, and $a/\Lambda=0.5$ in (a) and 0.75 in (b).

$$B=i\sin(\theta_{PQ\oplus}-\theta_{PQ\ominus}+\phi)e^{i(\theta_{PQ\oplus}+\theta_{PQ\ominus}+\phi)},\tag{24}$$

$$R_\pm=\frac{2\sqrt{\pi}Qb_\pm e^{i\theta_{PQ\oplus}}}{\nu_1 l(f_+b_++f_-b_-)f_QK^2(\eta-i\pi)},\tag{25}$$

where b_+/b_-, η, and ϕ are defined in Eqs. (18), (19), and (22). Thus we have obtained analytic forms of A, B, and $R_\pm$ as functions of (P,Q) or (K,Θ), using the quantities $K_\pm$, $f_\pm$, f_Q, and $\theta_{PQ\oplus,\ominus}$, which are associated with the eigenmodes for the empty lattice case (see Appendix A). It should be noted that the solution has a nonperturbative form in the coupling constants $\nu_{1,2}$.

E. Numerical examples

In the preceding subsections, we have derived a formal solution of the Maxwell equation (6), which is summarized in Fig. 3 with Eqs. (23), (24), and (25). Now we visualize the results at fixed parameters (see caption of Fig. 4) as functions of (K,Θ).

1. K dependence of η

First, we show the K dependence of η at several Θ in Fig. 4. The parameter a/Λ is set to 0.5 in Fig. 4(a) and 0.75 in 4(b), respectively. The qualitative difference between them is that the parameter ν_2 (coupling constant between two waveguide modes b_{P+G} and b_{P-G}) is zero for $a/\Lambda=0.5$ and nonzero for $a/\Lambda=0.75$. The following rewriting of η from Eq. (19) is helpful for understanding Fig. 4:

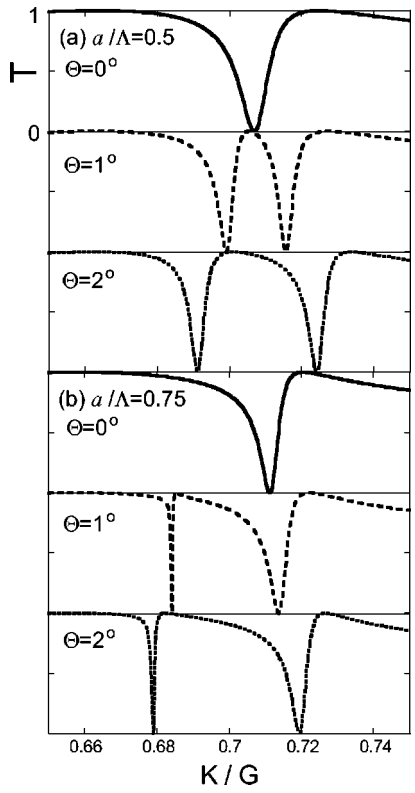

FIG. 5. Transmission spectrum $T(K)$ at $\Theta=0°, 1°$ and $2°$. The same parameters are used as in Fig. 4.

$$\eta=\frac{\cos\Theta}{\nu_1^2 l K^3 f_Q^2 f^2}\left[-(1+\nu_2 f^2)K^2+\frac{K_+^2+K_-^2}{2}+\frac{(K_+^2-K_-^2)^2/4}{(1-\nu_2 f^2)K^2-(K_+^2+K_-^2)/2}\right], \tag{26}$$

where $f_\pm$ are approximated by the K-independent constant f. $K_\pm$ are dependent on K for $\Theta\neq 0$, but they are approximated by $K_\pm \simeq G/\sqrt{\epsilon_s}\pm G\sin\Theta/\epsilon_s$ for small incident angle Θ. Then it is easily understood that the first and second terms in the bracket of Eq. (26) is almost insensitive to Θ, while the third one is proportional to $\sin^2\Theta$. Thus, for $\Theta\neq 0$, the third term is superposed to the curve for $\Theta=0$ (solid curves in Fig. 4).

2. Transmittivity $T=|A|^2$

Next, we proceed to discuss the transmittivity $T=|A|^2$, which is plotted in Fig. 5. As indicated by Eqs. (22) and (23), the dips in the transmission spectrum are formed where $\eta(K)$ changes sign. Denoting the solutions of $\eta(K)=0$ by K_1 and K_2 $(K_1<K_2)$, the dips locate around K_1 and K_2, and their widths are roughly evaluated by $\Delta K_{1(2)} \simeq 2\pi|\mathrm{d}\eta/\mathrm{d}K|^{-1}_{K=K_{1(2)}}$, which is roughly proportional to ν_1^2.[6]

For $\Theta=0$, there appears a single wide dip, irrespective of $a/\Lambda=0.5$ or 0.75. The qualitative difference between the two cases becomes clear for $\Theta\neq 0$. In case of $a/\Lambda=0.5$ [see Fig. 5(a)], the dip splits into two dips of the same width. On the other hand, in the case of $a/\Lambda=0.75$ [see Fig. 5(b)], a narrow dip appears at K_1 besides a wide dip at K_2. As expected from Fig. 4(b) and the fact that ΔK is proportional to $|\mathrm{d}\eta/\mathrm{d}K|^{-1}$, the width of the wider dip is almost independent of Θ, but the width of the narrower one is sensitive to Θ (proportional to $\sin^2\Theta$).

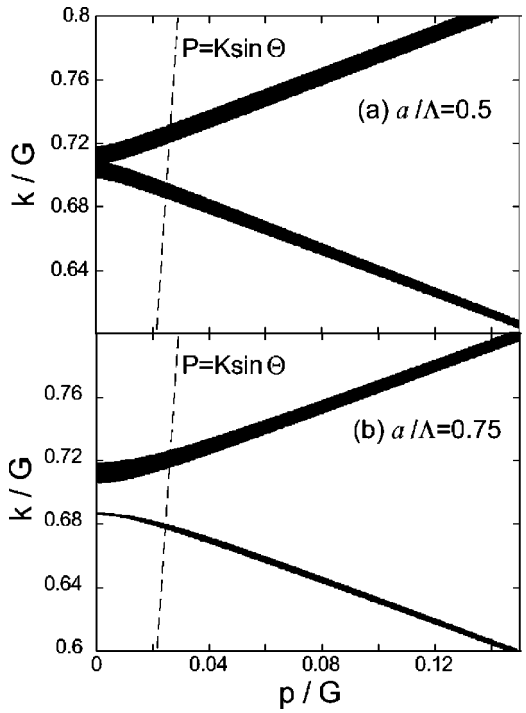

FIG. 6. Plot of the regions where $|\eta|<2\pi$ is satisfied, which can be interpreted as energy bands of waveguide modes. The width corresponds to the radiative width of the waveguide modes.

Comparison of rigorous numerical results[10,18] is carried out in Appendix B. We have confirmed there that the analytical results agree well with the numerical ones for $K/G<(1-\sin\Theta)/\cos^2\Theta$.

The regions satisfying $|\eta|<2\pi$ are plotted on the (P,K) plane in Fig. 6. These regions can be interpreted as energy bands of waveguide modes, which acquired finite width by coupling to radiation modes. There is no energy gap at $p=0$ for $a/\Lambda=0.5$ $(\nu_2=0)$, while a finite gap appears for $a/\Lambda=0.75$ $(\nu_2\neq 0)$; it is easily confirmed from Eq. (19) that the gap is proportional to $|\nu_2|$. Dips in the transmittivity appear at the intersections of the energy band and the line $P=K\sin\Theta$.

3. Excitation efficiency $R_\pm$ of waveguide modes

Finally, we discuss the excitation efficiency $R_\pm$ of waveguide modes. The absolute value and the phase of $R_\pm$ are shown in Figs. 7. For $\Theta=0$ (solid curves in Figs. 7), R_+ is equal to R_-, as expected from the symmetry. $|R_\pm|$ has a single peak at the dip energy in the transmittivity, accompanying gradual change of the phase by π.

R_+ (broken curves) and R_- (dotted curves) are no more equal for $\Theta\neq 0$. Interestingly, $R_{+(-)}$ becomes zero at $K=K_{-(+)}/\sqrt{1-\nu_2}$, which is reflected in the dips in $|R_\pm|$ (due

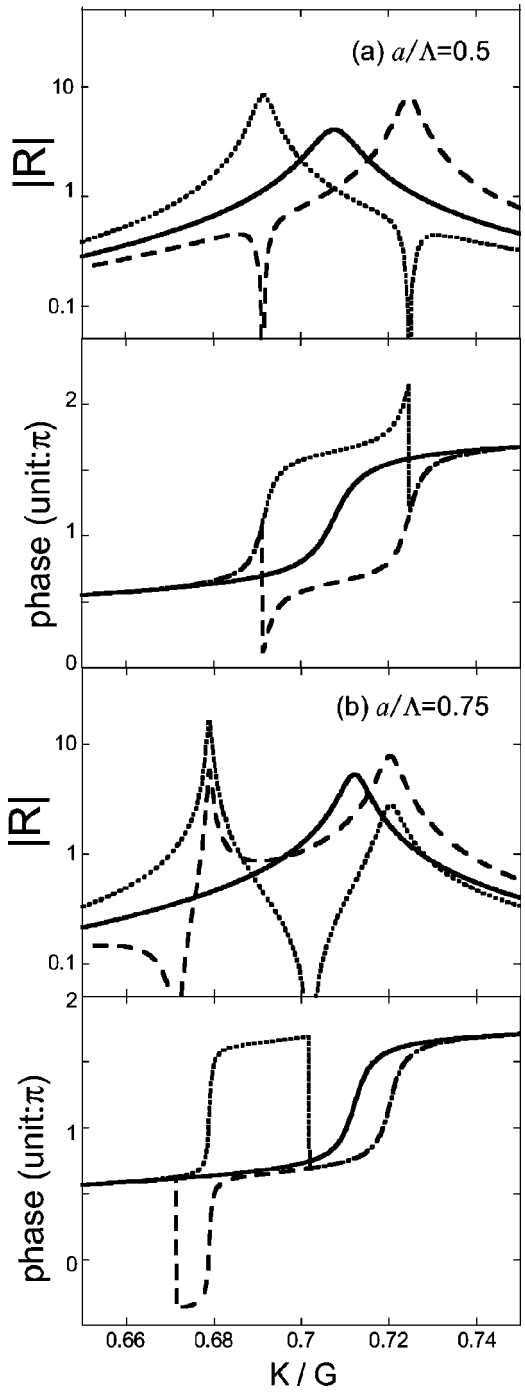

FIG. 7. Absolute values and phases of $R_+(=R_-)$ at $\Theta=0°$ (solid curve), R_+ at $\Theta=2°$ (broken curve), and R_- at $\Theta=2°$ (dotted curve). a/Λ is 0.5 in (a), and 0.75 in (b).

to logarithmic plot) and also in the discontinuous jumps by π in the phases. R_+ and R_- are out of phase between $K_-/\sqrt{1-\nu_2}$ and $K_+/\sqrt{1-\nu_2}$, and are in phase outside. In the case of $a/\Lambda=0.5$, $|R_{+(-)}|$ has a single peak at $K_{2(1)}$ and is almost zero at $K_{1(2)}$. This implies that the propagating wave with $p=P+G$ $(P-G)$ is excited at $K_{2(1)}$. Contrarily, in the case of $a/\Lambda=0.75$, $|R_\pm|$ have peaks at both $K=K_1$ and K_2. As is observed in Fig. 7(b), R_+ and R_- are in phase at K_1 and out of phase at K_2. This implies that the standing wave with $\cos Gx$ $(\sin Gx)$ type is excited at $K_{2(1)}$. The phases of $R_\pm$ change by π around both peaks; the change is gradual at K_2 and abrupt at K_1. This difference is related to the stability of the excited waves against the width in P, which will be discussed in the next section.

4. Comment on the case of $a/\Lambda<0.5$

We briefly comment on the cases of $a/\Lambda<0.5$, where ν_2 takes a positive value. In this case, a wide (narrow) dip appears at $K_{1(2)}$ in the transmission spectrum, where the standing wave of $\cos Gx$ $(\sin Gx)$ type is excited. This implies that the standing wave of $\cos Gx$ type has lower energy than the $\sin Gx$ type, contrary to the cases of $a/\Lambda>0.5$. This is because the $\cos Gx$ type covers the region of larger dielectric constant more effectively than the $\sin Gx$ type [compare $\int dx X(x)\cos^2 Gx$ and $\int dx X(x)\sin^2 Gx$].[19]

IV. EFFECT OF WIDTH IN P

In the previous section, we discussed the optical response of a PCS for plane wave incidence. However, in real situations, the finite width is introduced in P (x component in the wave vector) by several reasons such as finiteness of the periodic structure in the x direction, disorder in the periodic structure, and so on. In this section, we discuss the effect of finite width ΔP, introduced by the finiteness of the diameter of the incident wave for example.

We employ the following form for the incident wave, which has a finite diameter W in the x direction:

$$E^{(i)}(x,z)=w(x)e^{i(P_0x+Qz)} \tag{27}$$

$$=\int dp\, w(p-P_0)e^{i(px+Qz)}, \tag{28}$$

where $w(x)$ is a normalized ($\int w^2(x)dx=1$) Gaussian with width $\Delta x=W/2$, and $w(p-P_0)$ is its Fourier transform. They are given, respectively, by

$$w(x)=\left(\frac{8}{\pi W^2}\right)^{1/4} e^{-(2x/W)^2} \tag{29}$$

and

$$w(p-P_0)=\left(\frac{W^2}{32\pi^3}\right)^{1/4} e^{-[W(p-P_0)/4]^2}. \tag{30}$$

Thus, $w(p-P_0)$ is also a Gaussian with width $\Delta P=4/W$, and is normalized by $\int dp\, w^2(p-P_0)=(2\pi)^{-1}$.

As shown in Eq. (28), the incident wave is the superposition of plane waves. The transmitted wave $E^{(t)}(x,z)$ and the excited waveguide modes $E^{(\pm)}$ are therefore given by

$$E^{(t)}(x,z)=\int dp\, w(p-P_0)A(p,Q)e^{i(px+Qz)} \tag{31}$$

and

$$E^{(\pm)}(x,z)=\int dp\, w(p-P_0)R_\pm(p,Q)e^{i(p\pm G)x}\cos(\pi z/2l). \tag{32}$$

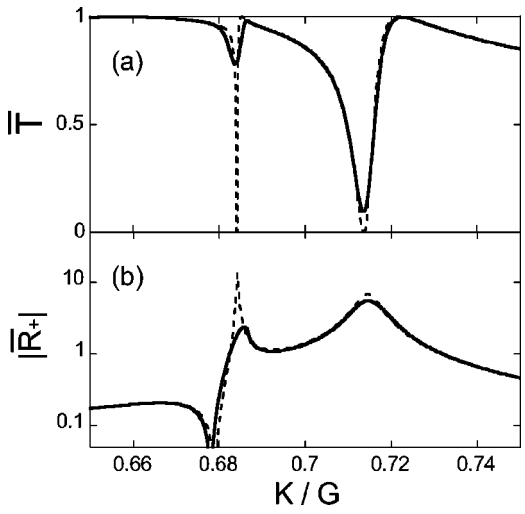

FIG. 8. Effect of ΔP in (a) transmittivity $\overline{T}$ and (b) $|\overline{R}_+|$, for $a/\Lambda=0.75$ and $\Theta=1°$. The solid (dotted) curve corresponds to $W=100\Lambda$ $(W=\infty)$ case.

Transmittivity $\overline{T}$ is given by the ratio of transmitted energy flow to that of the incident wave. Using the z component of the Poynting vector $S_z=(\mathrm{i}E\partial_z E^*+\mathrm{c.c.})/(\mu_0 cK)$, $\overline{T}$ is given by $\overline{T}=(\int_{z=-\infty}\mathrm{d}x S_z^{(\mathrm{i})})/(\int_{z=\infty}\mathrm{d}x S_z^{(\mathrm{t})})$, which is reduced with Eqs. (28) and (31) to

$$\overline{T}=2\pi\int \mathrm{d}p w^2(p-P_0)|A(p,Q)|^2, \tag{33}$$

i.e., averaging the transmittivity of the plane wave case with probability density $2\pi w^2(p-P_0)$. Numerical examples are shown in Figs. 8(a), where it is demonstrated that sharp dips observed in the plane wave case become shallower, which reproduces the experimental spectrums.[8,9]

As for the excitation efficiency of waveguide modes, we employ the ratio $\overline{R}_\pm$ of the amplitude of the waveguide mode to that of the incident wave, at $x=z=0$. It is given by

$$\overline{R}_\pm=(8/\pi W^2)^{-1/4}\int \mathrm{d}p w(p-P_0)R_\pm(p,Q), \tag{34}$$

which reduces to $R_\pm$ in the limit of $W\to\infty$. $|\overline{R}_+|$ is plotted as an example in Figs. 8(b). For $\Delta P=0$, sharp and wide peaks appear at $K=K_1$ and K_2, respectively. As ΔP is increased, while the wide peak is not altered significantly, the sharp peak become smaller, indicating the fragility to ΔP. This can be understood by considering the phase of R_+. As observed in Figs. 7(b), the phase of R_+ is sensitive to (P,Q) around K_1 but not so sensitive around K_2. Thus, the excited waves interfere destructively at K_1 in Eq. (34) if ΔP is considerably large.

V. SUMMARY

We have considered the optical response of a one-dimensional PCS, which has a structure sketched in Fig. 1. In the low frequency region where diffraction of the incident wave into other radiation modes does not occur, the Maxwell equation (6) has been reduced to a Fano-type problem with one continuum (radiation modes with $p=P$) and two discrete states (waveguide modes with $p=P\pm G$), as described in Fig. 2. The solution for a plane wave incidence is summarized in Fig. 3 with Eqs. (23), (24), and (25). The transmittivity $T=|A|^2$ and the amplitude of the excited waveguide modes $R_\pm$ are plotted in Figs. 5 and 7 as functions of the incident angle Θ and the wave number K of the incident wave. We have also discussed the effect of finite width in P (x component of the incident wave vector), which is inevitable in real experimental situations. It is demonstrated that the sharp dips in the transmittivity spectrum expected in the infinite plane wave case become duller as ΔP increases.

ACKNOWLEDGMENT

The author is grateful to E. A. Muljarov, N. A. Gippius, S. G. Tikhodeev, and T. Ishihara for fruitful discussions. The computation in this study was partly performed on a supercomputer operated by Computer and Information Division, the Institute of Physical and Chemical Research (RIKEN). This research was partially supported by the Ministry of Education, Science, Sports and Culture, Grant-in-Aid for Encouragement of Young Scientists, 13740193, 2001.

APPENDIX A: FORMS OF $F_{pq\sigma}(Z)$

In this appendix, we discuss the forms of $f_{pq\sigma}(z)$ which satisfy Eqs. (8) and (9). Equation (8) is equivalent to the Schrodinger equation for a one-dimensional particle in quantum well. Bound solutions $(q^2<0)$ correspond to waveguide modes, while unbound ones $(q^2>0)$ correspond to radiation modes. As for the radiation modes, $f_{pq\oplus}(z)$ and $f_{pq\ominus}(z)$ have the following forms:

$$f_{pq\oplus}(z)=\sqrt{\frac{2}{L}}\times\begin{cases}A_{pq\oplus}\cos(\tilde{q}|z|+\theta'_{pq\oplus}) & (|z|<l),\\ \cos(q|z|+\theta_{pq\oplus}) & (l<|z|),\end{cases} \tag{A1}$$

$$f_{pq\ominus}(z)=\sqrt{\frac{2}{L}}\times\begin{cases}A_{pq\ominus}\sin(\tilde{q}z) & (|z|<l),\\ (z/|z|)\sin(q|z|+\theta_{pq\ominus}) & (l<|z|),\end{cases} \tag{A2}$$

where $\tilde{q}^2=(\epsilon_s-1)p^2+\epsilon_s q^2$. The delta function in $\epsilon_1(z)$ affects only the even-parity modes, which results in $\theta'_{pq\oplus}=\arctan[\epsilon_a d a(p^2+q^2)/2\Lambda\tilde{q}]$. The amplitudes $A_{pq\oplus,\ominus}$ inside the slab and the phase shifts $\theta_{pq\oplus,\ominus}$ are determined by the continuity condition of f and $\mathrm{d}_z f$ at $z=\pm l$. For example, $A_{pq\oplus}$ is given by $A^2_{pq\oplus}=[\cos^2(\tilde{q}l+\theta_{pq\oplus})+(\tilde{q}/q)^2\sin^2(\tilde{q}l+\theta_{pq\oplus})]^{-1}$.

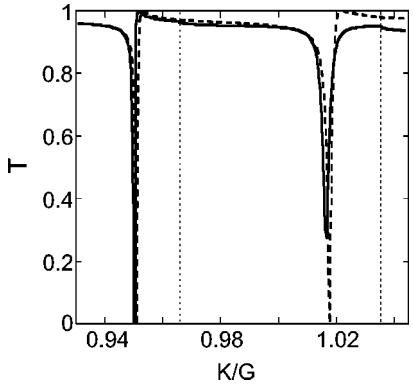

FIG. 9. Comparison of the transmissivities: the rigorous numerical result (solid curve) and the analytic result (broken curve). The vertical dotted lines show $K/G=(1-\sin\Theta)/\cos^2\Theta$ and $(1+\sin\Theta)/\cos^2\Theta$. The parameters are chosen as $\epsilon_s=1$, $\epsilon_a=5$, $d/\Lambda=0.02$, $a/\Lambda=0.75$, and the incident angle $\Theta=2°$. In $K/G<(1-\sin\Theta)/\cos^2\Theta$, the two results are in good agreement, while in $K/G>(1-\sin\Theta)/\cos^2\Theta$, deviation due to diffraction to another radiation modes appears.

As for the waveguide modes belonging to the lowest branch, their parity is even regardless of p. The mode function is proportional to $\cos(\tilde{q}|z|+\theta')$ inside the slab, and to $\exp[-|q||z|]$ outside of the slab. (If p is larger than $-\sqrt{\epsilon_s/4(\epsilon_s-1)}+\sqrt{\epsilon_s/4(\epsilon_s-1)+2\epsilon_s l\Lambda/\epsilon_a d a}$, the mode function inside the slab is proportional to $\cosh(\tilde{q}'|z|+\theta')$, where $\tilde{q}'=\sqrt{-\tilde{q}^2}$.) From the boundary condition at $z=0$ and l, $q^2(<0)$ is determined as a function of p, and $f_p(0)$ is determined after normalization.

APPENDIX B: COMPARISON TO RIGOROUS NUMERICAL RESULTS

In this appendix, we compare the analytic results of this study to the rigorous numerical results obtained by the S-matrix based method.[10] As an example, we plot in Fig. 9 the transmissivities T calculated by the numerical method (solid curve) and by the analytic results in this study (broken curve). The vertical dotted lines show $K/G=(1-\sin\Theta)/\cos^2\Theta$ and $(1+\sin\Theta)/\cos^2\Theta$.

In the energy region of $K/G<(1-\sin\Theta)/\cos^2\Theta$, in which region the analytic results in this study are applicable (see Sec. III B), the rigorous numerical results are well described by the formula (23), except for the slight energy shift in the waveguide mode. This shift originates in the off-resonant coupling between the waveguide mode ($p=P-G$) and the continuum ($p=P\pm G$), which is neglected in our treatment. This shift becomes less significant as ϵ_s-1 becomes larger, where the energy of the waveguide modes becomes lower. On the other hand, in $K/G>(1-\sin\Theta)/\cos^2\Theta$ $[(1+\sin\Theta)/\cos^2\Theta]$, the incident wave couples resonantly to the radiation modes with $p=P-G$ $[P+G]$. Then diffraction into those modes occurs, which results in cusps in the transmissivity obtained by rigorous numerical method (solid curve). In order to encompass this effect in the analytic method, inclusion of continua of radiation modes with $p=P\pm G$ is necessary, which is a straightforward extension of the present study.

*Electronic address: ikuzak@postman.riken.go.jp

[1] M. Born and E. Wolf, *Principles of Optics* (Cambridge, 1999).
[2] A. Sentenac, J-J. Greffet, and F. Pincemin, J. Opt. Soc. Am. B **14**, 339 (1997).
[3] S.G. Johnson, S. Fan, P.R. Villeneuve, J.D. Joannopoulos, and L.A. Kolodziejski, Phys. Rev. B **60**, 5751 (1999).
[4] E. Chow, S.Y. Lin, S.G. Johnson, P.B. Villeneuve, J.D. Joannopoulos, J.R. Wendt, G.A. Vawter, W. Zubrzycki, H. Hou, and A. Alleman, Nature (London) **407**, 983 (2000).
[5] T. Ochiai and K. Sakoda, Phys. Rev. B **63**, 125107 (2001).
[6] T. Ochiai and K. Sakoda, Phys. Rev. B **64**, 045108 (2001).
[7] It should be noted that those waveguide modes that are not folded back into the light cone do not interact with the radiation modes and therefore do not acquire radiative width, even in the existence of the grating.
[8] T. Fujita, Y. Sato, T. Kuitani, and T. Ishihara, Phys. Rev. B **57**, 12 428 (1998).
[9] R. Shimada, A.L. Yablonskii, S.G. Tikhodeev, and T. Ishihara, IEEE J. Quantum Electron. **38**, 872 (2002).
[10] A.L. Yablonskii, E.A. Muljarov, N.A. Gippius, S.G. Tikhodeev, and T. Ishihara, J. Phys. Soc. Jpn. **70**, 1137 (2001).
[11] S.G. Tikhodeev, A.L. Yablonskii, E.A. Muljarov, N.A. Gippius, and T. Ishihara, Phys. Rev. B **66**, 045102 (2002).
[12] H. A. Haus, *Waves and Fields in Optoelectronics* (Prentice-Hall, New Jersey, 1984).
[13] W.P. Huang, J. Opt. Soc. Am. A **11**, 963 (1994).
[14] A. Yariv, *Optical Electronics in Modern Communications* (Oxford Univ. Press, New York, 1997).
[15] U. Fano, Phys. Rev. **124**, 1866 (1961).
[16] By this substitution, the interaction between odd parity modes is neglected, which is much smaller than that between even parity modes.
[17] This approximation is equivalent to neglecting $\mathrm{P}\int_0^\infty dq f_q^2/(q^2-Q^2)$, which is roughly estimated by $-(\epsilon_s-1)\sin(2\sqrt{\epsilon_s}lQ)/(8\epsilon_s Q)$.
[18] E. A. Muljarov (private communication).
[19] J. D. Joannopoulos, R. D. Meade, and J. N. Winn, *Photonic Crystals* (Princeton Univ. Press, New Jersey, 1995).